Investigation of Allosteric Linkages in the Regulation of Tryptophan Synthase: The Roles of Salt Bridges and Monovalent Cations Probed by Site-Directed Mutation, Optical Spectroscopy, and Kinetics[†]

Eilika Weber-Ban,[‡,§] Oscar Hur,[§] Candy Bagwell,[§] Utpal Banik,[‖,⊥] Li-Hong Yang,[‖,#] Edith W. Miles,[‖] and Michael F. Dunn*[,§]

Department of Biochemistry, University of California at Riverside, Riverside, California 92521, and The National Institutes of Health, Bethesda, Maryland

ABSTRACT: The tryptophan synthase bienzyme complex is the most extensively documented example of substrate channeling in which the oligomeric unit has been described at near atomic resolution. Transfer of the common metabolite, indole, between the α- and the β-sites occurs by diffusion along a 25-Å-long interconnecting tunnel within each αβ-dimeric unit of the $\alpha_2\beta_2$ oligomer. The control of metabolite transfer involves allosteric interactions that trigger the switching of αβ-dimeric units between open and closed conformations and between catalytic states of low and high activity. This allosteric signaling is triggered by covalent transformations at the β-site and ligand binding to the α-site. The signals are transmitted between sites via a scaffolding of structural elements that includes a monovalent cation (MVC) binding site and salt bridging interactions of βLys 167 with βAsp 305 or αAsp 56. Through the combined strategies of site-directed mutations of these amino acid residues and cation substitutions at the MVC site, this work examines the interrelationship of the MVC site and the alternative salt bridges formed between Lys β167 with Asp β305 or Asp α56 to the regulation of channeling. These experiments show that both the binding of a MVC and the formation of the Lys β167−Asp α56 salt bridge are important to the transmission of allosteric signals between the sites, whereas, the salt bridge between βK167 and βD305 appears to be only of minor significance to catalysis and allosteric regulation. The mechanistic implications of these findings both for substrate channeling and for catalysis are discussed.

The tryptophan synthase bienzyme complexes from enteric bacteria (*1−4*) provide a new paradigm for the investigation of structure−function relationships involving allosteric interactions wherein the functional role of allostery is the regulation of substrate channeling between consecutive enzymes within a metabolic pathway (*5, 6*). Studies of the three-dimensional structure of the bienzyme complex from *S. typhimurium* have shown that the α- and β-sites of each αβ dimeric unit of the tetrameric ($\alpha_2\beta_2$) bienzyme complex are connected by a 25-Å-long tunnel (*7*). Solution kinetic studies have established that the common metabolite, indole (Scheme 1), is transferred from the α-site to the β-site via this tunnel (Scheme 2A) (*5, 8, 9*). Allosteric regulation of channeling in this system involves the switching of the bienzyme complex between an open conformation state of

low activity and a closed conformation state of high activity, triggered by ligand binding to the α-site and covalent transformations at the β-site (*6, 10, 11−17*). The thermodynamic studies of Fan et al. (*18*) have shown that the conformational change between open and closed states is strongly temperature dependent. In the temperature region around room temperature, the relative stabilities of the open and closed states are similar, and consequently, the distribution between states can be altered through the binding of allosteric ligands. The coordination of the interconversion between open and closed states with catalytic events (Scheme 2B) at the α- and β-sites is essential to the efficient channeling of indole between the two active sites (*6*). The protein structural elements (Scheme 2A and Figure 1) so far identified as important to this allosteric communication include the following: (a) a lid consisting of two loop structures in the α-subunit (loops 2 and 6) that fold down over the α-active site to give a closed structure, trapping substrates inside (*10, 11, 16, 17*); (b) a monovalent cation (MVC)[1] site located in the β-subunit about 8 Å from the β-active site (the $Na^+/K^+/Cs^+$ site) (*14, 16, 18−21*); (c) a system of two alternative salt bridges involving the Lys at β167 (βK167) and either Asp β305 (βD305) or Asp α56 (αD56) (*16, 17, 22−24*); and (d) domain rotations in the β-subunit which, in effect, create a lid that closes down over the β-site to give a closed structure.

* Corresponding Author: Michael F. Dunn, Department of Biochemistry, University of California at Riverside, Riverside, CA 92521. Phone: 909-787-4235. FAX: 909-787-4434. E-mail: dunn@ucrac1.ucr.edu.

[§] University of California at Riverside.

[‖] The National Institutes of Health.

[‡] Present Address: Institute of Molecular Biology and Biophysics, ETH Hönggerberg HPK E3, 8093 Zürich, Switzerland.

[⊥] Present Address: Vanderbilt School of Medicine, Vanderbilt University, Nashville, TN. 37232.

[#] Present Address: National Cancer Institute, NIH, Bethesda, MD 20892-4255.

Scheme 1: Reaction Schemes Showing Reactants, Products, and Key Intermediates in the α- and β-Reactions Catalyzed by the Tryptophan Synthase Bienzyme Complex
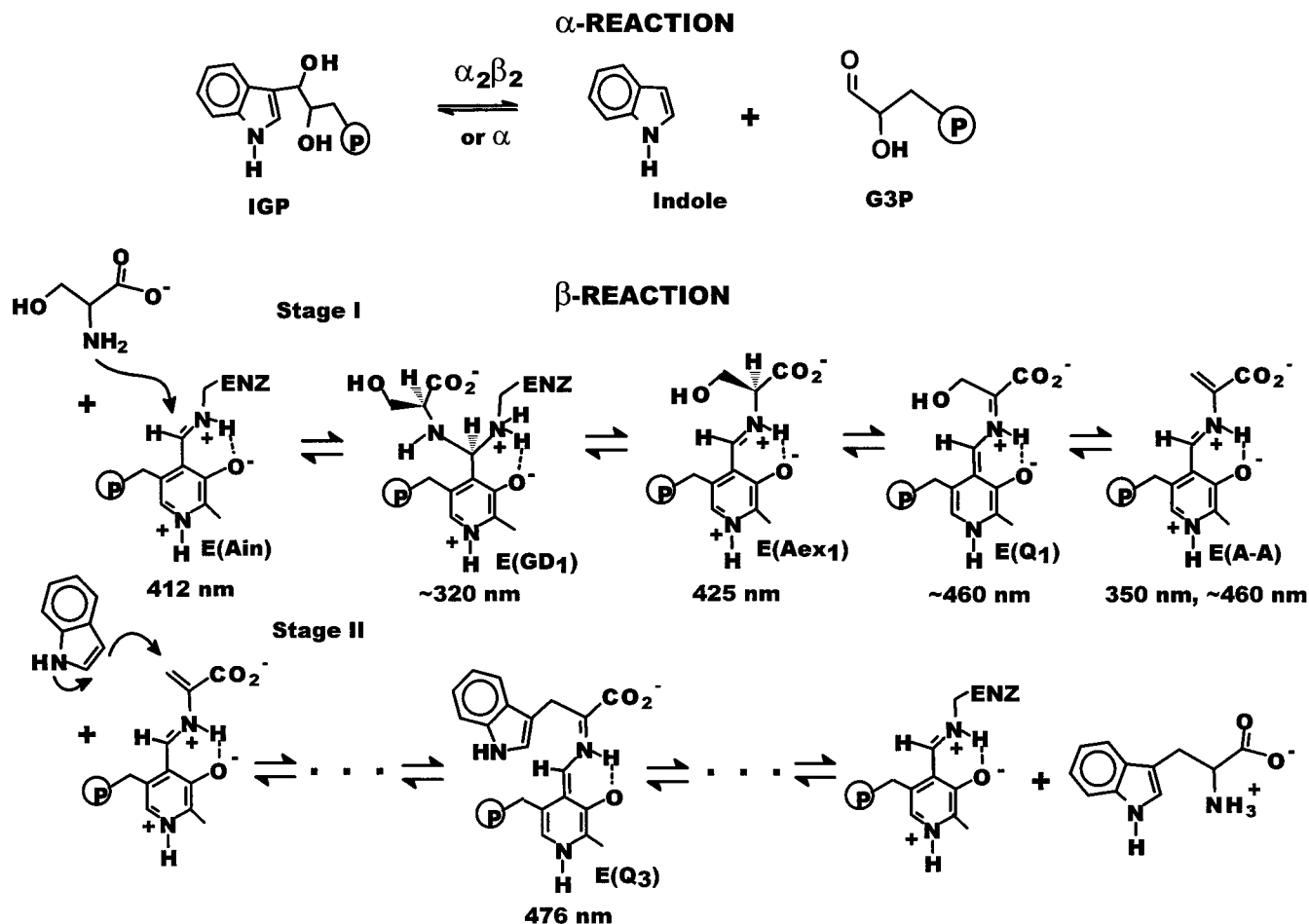
Crystallographic studies (*16*, *17*, *26*) and computer modeling analyses (*27*) indicate the rearrangement of these structural elements is linked to motions of loops in the α-subunit and domains in the β-subunits (Figure 1). The crystallographic description of the $Na^+/K^+/Cs^+$ MVC binding site (*16*) has demonstrated two conformations for that site and its immediate surroundings, leading to a rearrangement of residues extending from the β-site into the α-site. This rearrangement involves β-subunit residues βK167 and βD305 and α-subunit residue αD56. In one conformation, βK167 forms an intersubunit salt bridge to αD56 in the α-subunit (Scheme 2A and Figure 1, panels A and B), in the other

conformation, βK167 forms an intra-subunit salt-bridge to βD305 in the β-subunit (*16*) (Figure 1, panel A).

In this study, we present detailed comparisons of the effects of MVCs on the spectroscopic and catalytic properties of the wild-type enzyme and three mutant enzymes. These mutations involve the replacement of βK167 by Thr (βK167T) (*22*), the replacement of αD56 by Ala (αD56A), and the replacement of βD305 with Asn (βD305N) (*23*). As will be shown, the altered properties exhibited by these mutant enzymes give evidence that the βK167−αD56 intersubunit salt bridge is important for the transmission of allosteric signals in the bienzyme complex. Consequently, the switch from an inter- to an intra-subunit salt bridge appears to be an important component of the allosteric trigger responsible for communication between subunits. This work also shows there is a strong synergism between binding interactions at the MVC site, the formation of alternative salt bridges to support allosteric communication between sites, ligand binding to the α-site, and the catalytic activities of the α- and β-sites.

To make this presentation as straightforward as possible, the data are organized by experiment type with the behavior of each enzyme species described within the context of the influence of the various effectors (MVCs and GP). The discussion of these data then is organized to compare the MVC-free, Na^+, K^+, and NH_4^+ forms, and the Na^+ and GP forms, of the wild-type and mutant enzymes. This cross comparison of the effects of the mutations with the influence

---

[1] Abbreviations: $α_2β_2$, the tryptophan synthase bienzyme complex; $β_2$, the β-subunit dimer; βK167T, the tryptophan synthase mutant in which β-subunit Lys 167 is replaced by Thr; βD305N, the mutant in which β-subunit Asp 305 is replaced by Asn; αD56A, the mutant in which α-subunit Asp 56 is replaced by Ala; IGP, 3-indole-D-glycerol 3′-phosphate; IPP and 5-F-IGP, 3-indole-propanol 3′-phosphate and 3-[5-fluoro-indole]-propanol 3′-phosphate, respectively; G3P, D-glyceraldehyde 3-phosphate; GP, α-glycerolphosphate; L-Ser and D,L-Ser, L-serine and D,L-serine, respectively; L-Trp, L-tryptophan; PLP, pyridoxal-5-phosphate; the various covalent forms of PLP-bound serine at the β-site (see Scheme 1) are designated as follows: E(Ain), the internal aldimine (Schiff base); E(GD$_1$), the first gem diamine species; E(Aex$_1$), the L-Ser external aldimine (Schiff base); E(Q$_1$), the L-Ser quinonoid; E(A-A), the α-aminoacrylate Schiff base; E(Q$_2$), the quinonoid formed initially in the Michael addition of indole with E(A-A); E(Q$_3$) the quinonoid formed by abstraction of a proton from E(Q$_2$); E(Aex$_2$), the L-Trp external aldimine (Schiff base); E(GD$_2$), the L-Trp gem diamine; KIE, kinetic isotope effect; SWSF single-wavelength stopped-flow; PDB, protein data bank.

Scheme 2: (A) Cartoon Depicting Structural Elements Involved in Substrate Channeling and Allosteric Communication between the α- and β-sites of Tryptophan Synthase[a] and (B) Cartoons Showing the Open (Ellipse), Closed (Square), and Partially Closed (Octagonal) Conformations Proposed for Key Intermediates along the Catalytic Cycle of the αβ-reaction (6, 15, 20, 21)[b]

A

B
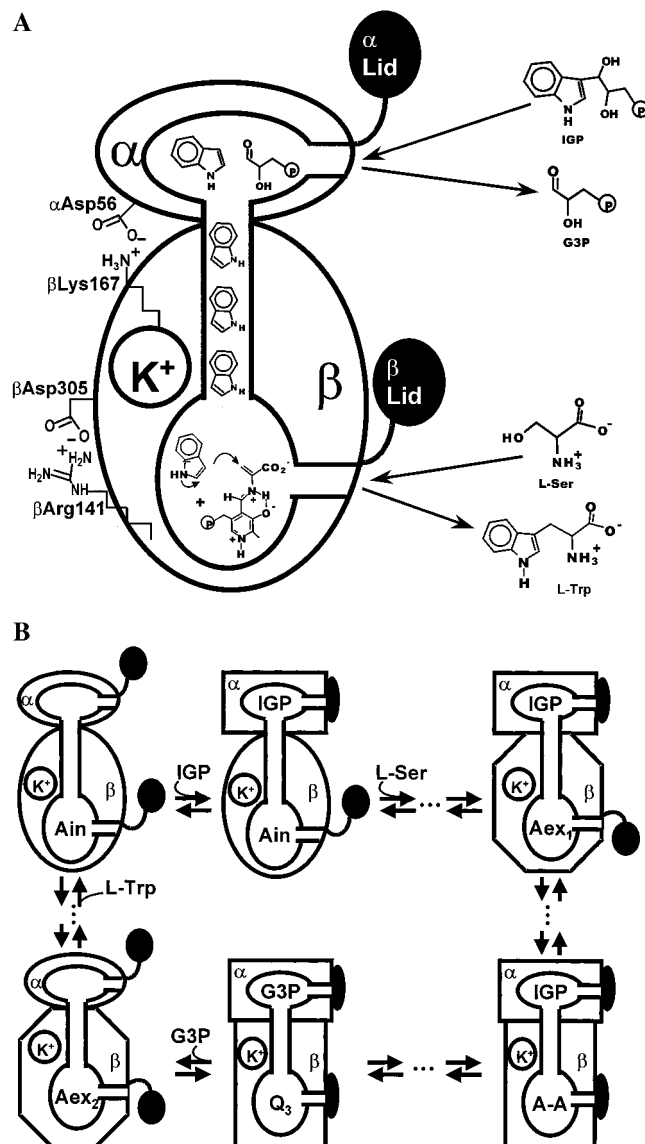
[a] The catalytic cycle is initiated by the binding of 3-indolyl-D-glycerol 3′-phosphate (IGP) to the α-site, and the reaction of L-Ser with PLP to form the α-aminoacrylate Schiff base, E(A—A), at the β-site. E(A-A) formation triggers an allosteric signal that activates cleavage of IGP at the α-site. The indole produced by cleavage of IGP diffuses through the 25-Å-long tunnel into the β-site where reaction with E(A-A) occurs. The products D-glyceraldehyde 3-phosphate and L-Trp are shown leaving their respective catalytic sites. Structural elements involved in transmission of the allosteric signal include the monovalent cation (MVC) site (shown occupied by K^+), and the amino acid residues αD56, βK167, βD305, and βR141, which form a lattice of salt bridging interactions that connect the α- and β-sites, and the lid structures that close down over the sites to form closed conformations. Redrawn from Pan et al. (6) with permission. [b] The lids that close the α- and β-sites are shown as black ellipses. Ligation states of the α-site and covalent states of the β-site are indicated by the acronyms defined in Scheme 1. Redrawn from Pan et al. (6) with permission.

of the effectors serves to identify roles played by the MVC site and by protein residues βK167, βD305, and αD56 in

the communication of allosteric signals between the α- and β-sites.

MATERIALS AND METHODS

Materials. The preparation of wild-type enzyme, substrates, effectors, buffers and the sources of reagents used in this study have been previously described (20). To remove MVCs, the enzymes were dialyzed against pH 7.8 metal ion-free 50 mM triethanolamine (TEA) buffer prior to usage as previously described (14, 20, 21). The various MVC-substituted enzyme species were prepared by adding the desired MVC to the MVC-free enzyme. The following mutants were prepared by previously published methods βK167T (22), βD305N (23), and αD56A (24).

Optical Spectroscopy and Enzyme Assays. All of the experimental work reported herein was carried out at 25.0 ± 2.0° C and pH 7.8 in 50 mM TEA buffer. Optical spectroscopy, activity measurements, fluorescence stopped-flow kinetic studies, single-wavelength stopped flow (SWSF), and rapid-scanning measurements were performed as previously described (20, 28−34). Single-wavelength time courses were fit by the Marquardt−Levenberg algorithm to equations of the general form of eq 1:

$$A = A_0 \pm \sum A_n \exp\left(\frac{-t}{\tau_n}\right) \quad (1)$$

where A and A_0 are the absorbance values at time t and at time infinity, A_n is the amplitude of the nth relaxation, τ_n.

Titration Studies. The dependence of the amount of quinonoidal species formed in the reaction of E(A-A) with indoline as a function of NH_4^+ concentration was determined by rapidly mixing solutions of varying NH_4^+ concentration containing preincubated enzyme and L-Ser with indoline in the stopped-flow apparatus and determining the maximum amplitude of the absorbance change at 464 nm.

RESULTS

Influence of Allosteric Effectors on the Distribution of Intermediates. (a) Static UV/Vis Absorbance Measurements for Wild-Type Tryptophan Synthase. There is an extensive literature describing the influence of allosteric effectors on rates and equilibria for the reactions of wild-type and mutant tryptophan synthases both with L-Ser (stage I of the β-reaction, Scheme 1), and with L-Ser and indoline (an indole analogue) (5, 6, 8, 10−15, 19−21). Indoline reacts rapidly and reversibly with E(A-A) to form a quasi-stable quinonoid, $E(Q)_{Indoline}$ (λ_{max} 464 nm), which then very slowly is converted to dihydroiso-L-tryptophan (eq 2) (35).
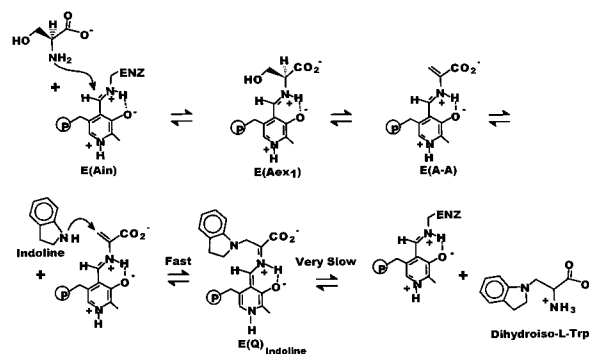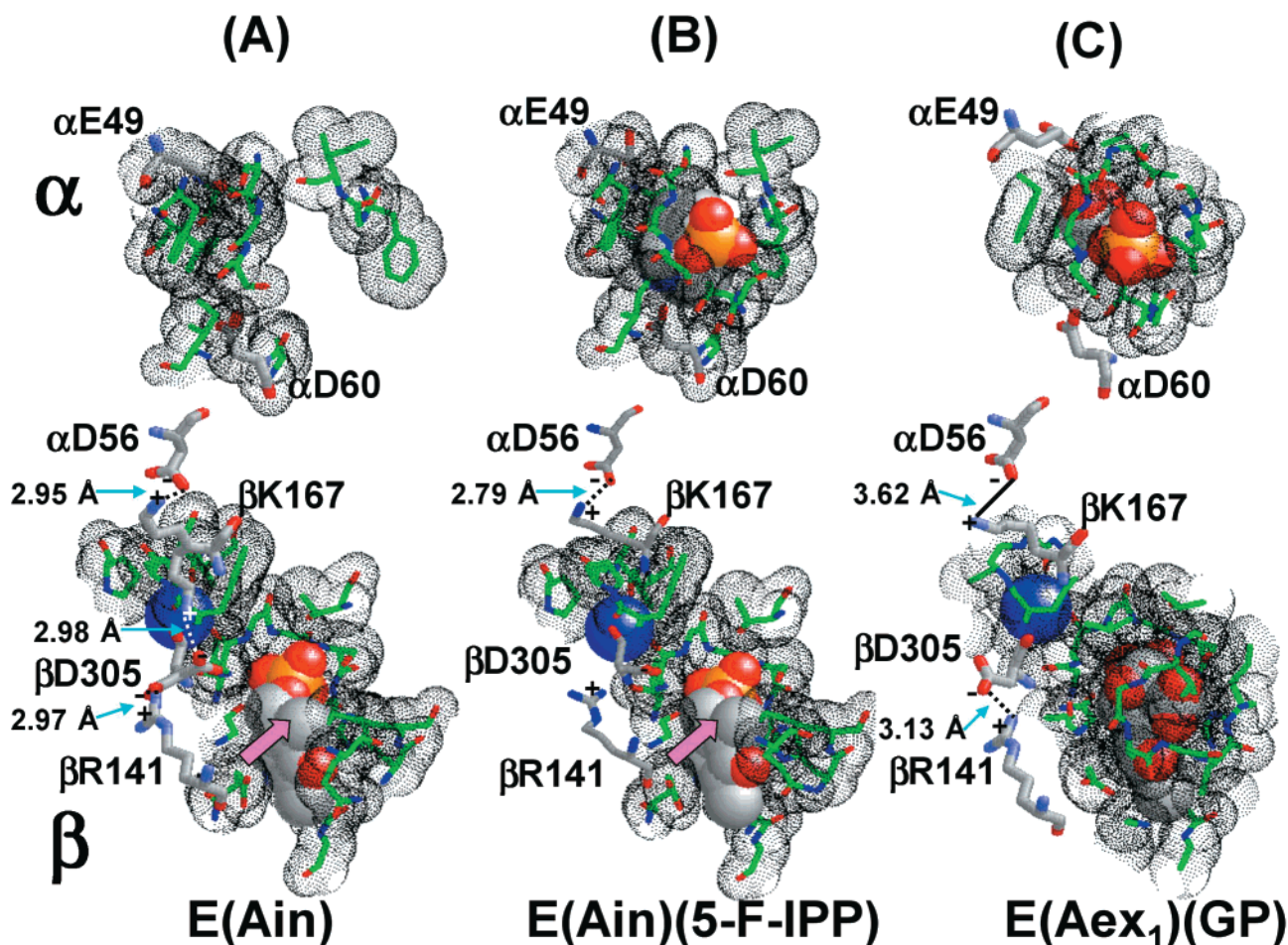
FIGURE 1: Structural details of the α- and β-sites and the MVC $Na^+/K^+/Cs^+$ site occupied by Na^+ (blue ball) for (A) E(Ain) where both the α- and β- sites are open (PDB file 1BKS), (B) the complex of 5-fluoro-IPP with E(Ain) where the α-site is closed and the β-site is open (PDB file 1A50), and (C) the complex of GP with the βK87T mutant of E(Aex₁) where both the α- and β-sites are closed. The route of access into the β-site is indicated in panels A and B by the large magenta arrows. In panels B and C, those residues within 5.0 Å of the α- and β-site ligands are represented as green wire frame structures with oxygen red and nitrogen blue, and with the van der Waals surfaces are shown as black dots. The ligands are shown in space filling representations with atom types designated by the CPK coloring convention. In panel A, using the same conventions, the same residues found surrounding the ligands in panel B are shown except for αT183 and αG184. These two residues are part of a disordered loop in the E(Ain) structure. The side chains of βK167 and βD305 are each shown in two different conformations; in one conformation, βK167 forms a salt bridge with αD56 and βD305 forms a salt bridge with βR141, in the other conformation, βK167 forms a salt bridge to βD305. In all three structures, the α-active site catalytic residues, αE49 and αD60, are shown together with the salt-bridge-forming residues, αD56, βK167, βD305, and βR141, in stick representations with CPK colors. The interatomic distances for potential salt-bridging interactions (solid line) are given, and, where indicated by the interatomic distances, H-bonding interactions between these residues are shown as dashed lines.

At pH 7.8 and room temperature (*18*), the distribution of intermediates formed in these reactions has been shown to be remarkably sensitive both to the nature of the allosteric effector and to the nature of the mutation (see Figure 2 and Table 1). Figure 2, panel A, presents a set of reference spectra (for comparison with the mutants described below) showing the effects of MVCs and GP on the reaction of wild-type enzyme with L-Ser in stage I. Figure 2, panel B, presents the corresponding set of reference spectra for the reaction of wild-type enzyme with L-Ser and indoline. Spectral assignments are summarized in Table 1.

In stage I, E(A-A), with $\lambda_{max} = 350$ nm and a shoulder extending beyond 500 nm ($\lambda_{max} \sim 460$ nm, Table 1), is the predominant species formed both in the absence of effectors and in the presence of NH_4^+, or GP, or in the presence of both Na^+ and GP^2 (Figure 2, panel A). As evidenced by the presence of an absorbance band located at 425 nm, there are significant amounts of the E(Aex₁) species present at

equilibrium when the effector is either Na^+ or NH_4^+ or when Na^+ and GP both are bound.

The influence of MVCs and GP on the distribution of species formed in the reaction of wild-type enzyme with L-Ser and indoline is shown in Figure 2, panel B, and Table 1. Figure 2, panel B, shows that the yield of E(Q)ₗₙdoline is remarkably dependent upon the allosteric effector present. When no effectors are present, the yield of E(Q)ₗₙdoline is small and the absorption band at 350 nm indicates that most of the β-sites are in the form of E(A-A). The distribution of E(A-A) and E(Q)ₗₙdoline is shifted slightly toward E(Q)ₗₙdoline by the binding of either NH_4^+ or GP, whereas Na^+ or the

---

[2] The assignments of the UV/Vis absorption bands to the various PLP intermediates along the β-reaction pathway are well-established for tryptophan synthase (*31, 32*). These assignments are as follows: E(Ain), 412 nm; E(Ain)(S), 412 nm; E(Aex₁), 425 nm; E(Q), 460−480 nm; E(A-A), 350 nm with a shoulder to >500 nm; E(Aex₂), 414 nm (see also Table 1).
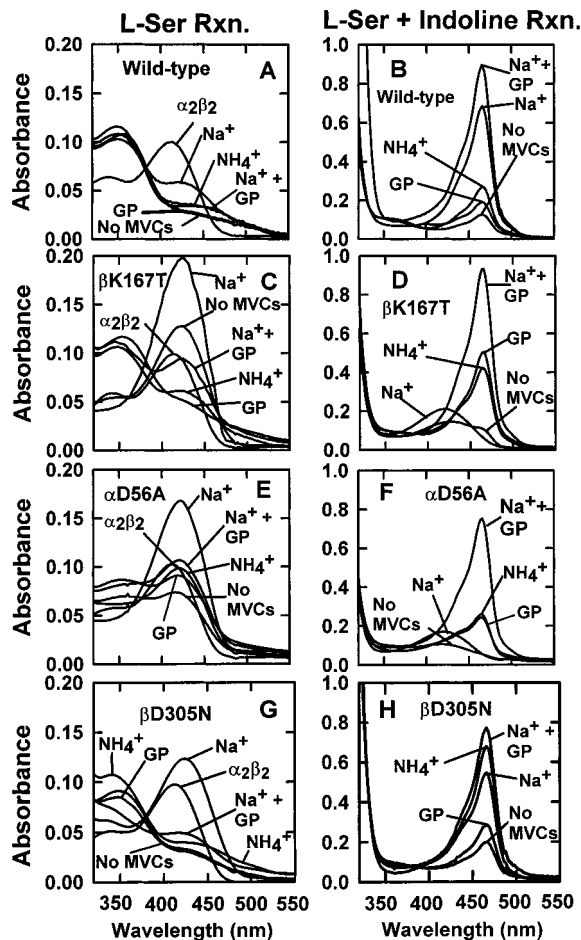
FIGURE 2: Comparison of static UV/Vis absorption spectra for the reaction of wild-type enzyme (A, B), the βK167T (C, D), the αD56A (E, F), and the βD305N (G, H) mutants with L-Ser (stage I) and with L-Ser and indoline both in the absence and in the presence of effectors. Spectra in panels A, C, E, and G were measured under the following conditions: E(Ain) before reaction, reaction with L-Ser in the absence of effectors (no MVCs), and reaction in the presence of the following effectors: 100 mM NaCl, 50 mM NH$_4$Cl, 50 mM MVC-free GP, or 200 mM NaCl and 50 mM GP. Spectra in panels B, D, F, and H for the reaction with L-Ser and indoline were measured under the same effector conditions as in panels A, C, E, and G. Conditions: [enzyme] = 8.3 μM, and [L-Ser] = 40 mM, and [indoline] = 4.5 mM when present, all in pH 7.8 TEA buffer and 25.0 $\pm$ 2.0° C.

combination of Na$^+$ and GP strongly shifts the distribution in favor of E(Q)$_{Indoline}$.

(b) Static UV/Vis Absorbance Measurements for βK167T. The effects of MVCs and GP on the equilibrium spectra obtained after reaction of βK167T with L-Ser in stage I, and after reaction with L-Ser and indoline are shown in Figure 2, panel C, and Figure 2, panel D. These spectra show that, in the absence of effectors, the mutant enzyme gives a mixture of E(Ain), and its Michaelis complex with L-Ser and E(Aex$_1$). The presence of Na$^+$ further shifts the equilibrium toward E(Aex$_1$), whereas NH$_4^+$ and the combination of Na$^+$ and GP gives equilibria consisting of comparable amounts of the E(A-A) and E(Aex$_1$) species, as seen with the wild-type enzyme. Addition of GP further shifts the equilibrium distribution of species toward E(A-A). In Figure 2, panel D, the effects of the same ligands were tested on the reaction of E(A-A) with indoline (35). A significant amount of E(Q)$_{Indoline}$ is only formed in the presence of NH$_4^+$, GP, or

GP and Na$^+$. Na$^+$ alone stabilizes E(Aex$_1$), and detectable amounts of E(Q)$_{Indoline}$ do not form in the presence of Na$^+$ alone. However, the highest yield of E(Q)$_{Indoline}$ results when both GP and Na$^+$ are present.

(c) Static UV/Vis Absorbance Measurements for αD56A. The reaction of αD56A with L-Ser (Figure 2, panel E) in the absence of effectors gives a mixture of E(Ain) and its Michaelis complex with L-Ser, and E(Aex$_1$), but little or no E(A-A) is formed. In the presence of 100 mM Na$^+$, E(Aex$_1$) is the predominating species, whereas, 50 mM NH$_4^+$, 50 mM GP, or 200 mM Na$^+$ and 50 mM GP gives distributions that favor E(Aex$_1$) with some E(A-A).

In the reaction of L-Ser and indoline with αD56A (Figure 2, panel F), only a trace of E(Q)$_{Indoline}$ is formed in the absence of effectors. Na$^+$ stabilizes E(Aex$_1$), and there is no indication of E(Q)$_{Indoline}$ in the spectrum. The yields of E(Q)$_{Indoline}$ in the presence of NH$_4^+$, GP, or the combination of Na$^+$ and GP are similar to the yield with wild-type enzyme. In contrast to the wild-type enzyme where the rates of E(Q)$_{Indoline}$ formation are rapid (both in the absence and in the presence of effectors), the reaction of the αD56A mutant in the absence of effectors is relatively slow ($t_{1/2} \sim$ 3 to 4 min) under the conditions of Figure 2, panel F. Although the presence of effectors speeds up the reaction, the rates of formation of E(Q)$_{Indoline}$ are noticeably slower than for the wild-type enzyme (*14, 21*).

(d) Static UV/Vis Absorbance Measurements for βD305N. The equilibrium distribution of intermediates formed in the reaction of βD305N with L-Ser, and in the reaction with L-Ser and indoline (Figure 2, panels G and H) are very similar to the wild-type enzyme (see Figure 2, panels A and B). In the L-Ser reaction (Figure 2, panel G), the equilibrium is shifted toward the E(Aex$_1$) species by Na$^+$, whereas NH$_4^+$ stabilizes E(A-A), as do GP and the combination of GP and Na$^+$. In the reaction with L-Ser and indoline, some E(Q)$_{Indoline}$ is formed in the absence of MVCs (Figure 2, panel H), but the proportion of the quinonoidal species formed is strongly enhanced by MVC binding. GP alone does not significantly stabilize E(Q)$_{Indoline}$.

Influence of Allosteric Effectors on Activity. (a) Wild-Type. Under the experimental conditions selected for these comparisons, the β- and $\alpha\beta$-reaction activities (calculated as the initial velocity divided by the total enzyme concentration, $v_i/[E_O]$) of the wild-type enzyme are strongly activated by the binding of MVCs (Figures 3, panels A and B), whereas the α-activity is somewhat suppressed (Figure 3C) (*20, 21*). Of the MVCs tested in this study, NH$_4^+$ is the best activator of the β-reaction (8-fold, Figure 3, panel A). Na$^+$ is the best activator of the $\alpha\beta$-reaction (10-fold, Figure 3, panel B), and the α-reaction (Figure 3, panel C) is inhibited by MVCs (to 33% of the MVC-free value by Na$^+$ and K$^+$ and to 18% by NH$_4^+$). The β-reaction is suppressed to 25% of the effector-free activity by the binding of MVC-free GP (Figure 3, panel A).

The extent to which the reaction of L-Ser at the β-site activates the α-site (see the β- and α-reaction, Scheme 1) is given by the $\alpha\beta/\alpha$ activity ratio. Figure 4 compares the influence of MVCs on this activation. In the absence of MVCs, there is almost no activation of the wild-type enzyme, whereas the MVCs all give enzyme complexes in which the α-reaction is strongly activated by the reaction of L-Ser at the β-site (Na$^+$, 30-fold; K$^+$, 26-fold; NH$_4^+$, 40-fold). This

Table 1: Summary of Spectral and Conformation State Assignments for Tryptophan Synthase[a]

β-site covalent state and α-site ligation[a]	PDB files[a]	long wavelength UV/Vis spectral bands[b] (nm)	α- and β-site conformation states[c]
β: Ain α: empty	1BKS; 1A5A (36); 1TTP (16); 1TTQ (16)	412	β: open α: open
β: Ain α: analogues	1A50 (26); 1A5B (36); 1BEU (44); 1C29 (37); 1C8V (37); 1C9D (37); 1CW2 (37); 1CX9 (37)	412	β: open α: closed
β: Aex$_1$ α: empty	1UBS (17)	425	β: partially closed α: open
β: Aex$_1$ α: analogues	2TRS (17); 2TSY (17)	425	β: closed α: closed
β: A$-$A α: analogue	1A5S (26)	350; ~460 (shoulder)	β: closed α: closed
E(Q)$_{Indoline}$		464	β: closed α: closed
β: Aex$_2$ α: empty	2TYS (17)	414	β: closed α: closed

[a] Based on Pan et al. (6) and the available X-ray structures taken from the Protein Data Base (PDB). Organic structures are drawn in Scheme 1 for the various intermediates identified along the β-reaction pathway.[1]   [b] Spectral assignments are taken from published data (1, 2, 5, 31, 32, 35). [c] β-Site conformation states are based on solution studies (5, 10−12, 15), and X-ray structure work (7, 16, 17, 26, 36, 37). Although the α-site appears to take up closed conformations when bound to IGP, G3P, or the analogue GP, activation of the α-site occurs only upon conversion of the β-site to the E(A-A) or E(Q) states (6, 12, 13).
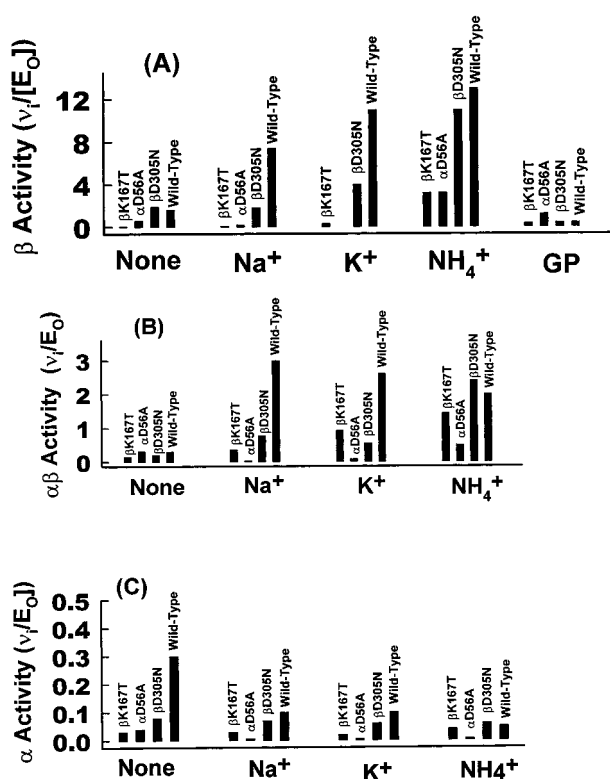

FIGURE 3: Bar graphs comparing the influence of effectors on the activities of the β-reaction (A), the $\alpha\beta$-reaction (B), and the α-reaction (C) of the wild-type, β K167T, αD56A, and βD305N enzyme species. Steady-state activities, expressed as $v_i/[E_O]$ with units of s^{-1}, were measured as previously described (14, 20, 21). Typical conditions were as follows: [enzyme] = 0.5 μM; β-reaction: [L-Ser] = 40 mM; [indole] = 0.2 mM; $\alpha\beta$-reaction: [L-Ser] = 40 mM; [IGP] = 0.2 mM; α-reaction: [IGP] = 0.2 mM. Where present, the effector concentrations were as follows: [NaCl] = 100 mM; [KCl] = 100 mM; [NH$_4$Cl] = 50 mM; [GP] = 50 mM. Error limits were estimated to be ± 15%. All activities were measured in pH 7.8 TEA buffer and 25.0 ± 2.0° C.

activation has been shown to be due to an allosteric interaction between the β- and the α-sites that switches the
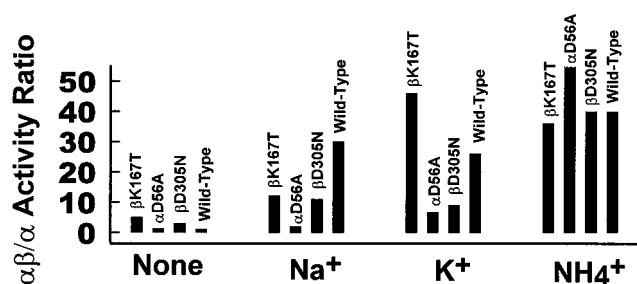

FIGURE 4: Bar graph comparing the influence of effectors on the ratio of the $\alpha\beta$- and α- activities ($\alpha\beta/\alpha$) of the wild-type, β K167T, αD56A, and βD305N enzyme species. Data taken from Figure 3. Error limits on activities were estimated to be ± 15%.

α-site from an inactive state to an active state triggered by the formation of the E(A-A) intermediate (12, 13).

(b) βK167T. The β-reaction activity ($v_i/[E]$) of the βK167T mutant enzyme in the absence of any effectors is very low (0.03 s^{-1}, 1.8% of wild-type activity in the absence of effectors) (Figure 3, panel A). The presence of Na$^+$ does not stimulate the activity of the β-reaction significantly, a fact that is in strong contrast with the behavior of wild-type enzyme where a 4- to 5-fold stimulation is found (Figure 3, panel A) (20, 21). The presence of K$^+$ stimulates the activity by ~10-fold. The presence of NH$_4^+$ stimulates the β-reaction activity by 107-fold (3.2 s^{-1}) and restores activity to a value that is 25% of the wild-type enzyme value in the presence of metal ions. Inorganic phosphate ion (data not shown) does not stimulate the β-reaction. The combination of both Na$^+$ and phosphate ion stimulates the β-reaction to about the same extent as K$^+$ alone (0.2 s^{-1}) (data not shown). The presence of metal-free GP stimulates the reaction to a similar extent (0.32 s^{-1}) (Figure 3, panel A). The combination of Na$^+$ and GP also restores a significant amount of activity, giving a 57-fold stimulation (1.7 s^{-1}).

Activity measurements for the $\alpha\beta$-reaction (Figure 3, panel B) show that in comparison to the MVC-free system, Na$^+$ is weakly activating (2.4-fold), while K$^+$ and NH$_4^+$ are more

Table 2: Summary of the Effects of MCV Binding on Relaxation Rate Constants for the Formation and Decay of the $E(Aex_1)$ Species in Reactions Catalyzed by the Wild-Type, βK167T, αD56A, and βD305N Mutant Enzymes

reaction	$1/\tau$ $(s^{-1})^{a,b}$	no MVCs	Na^+	K^+	NH_4^+	refs and figs
wild-type $\alpha_2\beta_2$ + L-Ser	$1/\tau_1$ (up)	200	900	660	420	*14, 20, 21*
	$1/\tau_2$ (up)		50–100			
	$1/\tau_3$ (down)	21	7	20	90	
wild-type $\alpha_2\beta_2$ + (L-Ser + Indole)	$1/\tau_1$ (up)	210	910	600	350	*14, 19, 20*
	$1/\tau_2$ (up)		50–100			
	$1/\tau_3$ (down)			30	100	
βK167T + L-Ser	$1/\tau_1$ (up)	100	750	620	–	Figure 5A
	$1/\tau_2$ (up)		68	110	270	
	$1/\tau_3$ (down)				5	
βK167T + (L-Ser + Indole)	$1/\tau_1$ (up)	94	740	522	340	Figure 5B
	$1/\tau_2$ (up)		95	97		
αD56A + L-Ser	$1/\tau_1$ (up)	94	360	600	250	Figure 5C
	$1/\tau_2$ (up		15.0	107		
	$1/\tau_3$ (down)	1.8			5.1	
αD56A + (L-Ser + indole)	$1/\tau_1$ (up)	120	390	240	150	Figure 5D
	$1/\tau_2$ (up		25	8.0		
	$1/\tau_3$ (down)	1.6			30	
βD305N + L-Ser	$1/\tau_1$ (up)	100	80		250	Figure 5E
	$1/\tau_2$ (down)	3	6		19	
	$1/\tau_3$ (down)	0.5–1			1	
βD305N + (L-Ser + indole)	$1/\tau_1$ (up)	95	90		220	Figure 5F
	$1/\tau_2$ (down)	1–1.5	5		60	

[a] Relaxation rate constants are taken from data collected under the conditions shown in Figure 5. Relaxations corresponding to formation of $E(Aex_1)$ (increasing fluorescence) are indicated as (up), and to decay of $E(Aex_1)$ (decreasing fluorescence) are indicated as (down). [b] Error limits in the absence of MVCs are estimated to be as follows: $1/\tau_1$, $\pm$ 10%; $1/\tau_2$, $\pm$ 5%; $1/\tau_3$, $\pm$ 20%. In the presence of Na^+, $1/\tau_1$, $\pm$ 15%; $1/\tau_2$, $\pm$ 15%; $1/\tau_3$, $\pm$ 5%. In the presence of K^+, $1/\tau_1$, $\pm$ 15%; $1/\tau_2$, $\pm$ 10%; $1/\tau_3$, $\pm$ 10%. In the presence of NH_4^+, $1/\tau_1$, $\pm$ 10%; $1/\tau_2$, $\pm$ 10%; $1/\tau_3$, $\pm$ 10%.

strongly activating (6- and 10-fold, respectively). The activity levels achieved are less than those found for the wild-type enzyme by 7- to 1.4-fold. Only NH_4^+ restores the activity to a level that is similar in magnitude to that of wild-type enzyme.

The α-activity exhibited by βK167T (Figure 3, panel C) was found to be essentially unaffected by MVCs. This mutation was found to suppress the α-activity to ~10% of the wild-type enzyme activity.

In the βK167T system, the allosteric effects of the L-Ser reaction on the activity of the α-site in the absence and in the presence of MVCs as measured by the $\alpha\beta/\alpha$ activity ratio are shown in Figure 4. In the absence of MVCs, there is only a 5-fold (0.03 to 0.15 s^{-1}) stimulation of the α-reaction due to the formation of the E(A-A) intermediate. In the presence of Na^+ ions, this stimulation is stronger (12-fold from 0.03 to 0.36 s^{-1}), while K^+ and NH_4^+ ions stimulate to a significant extent (51- and 36-fold respectively).

(c) αD56A. Figure 3, panel A, shows that in the β-reaction the MVC-free αD56A species is somewhat more active than is the βK167T species and gives turnover rates similar to the wild-type and βD305N mutant species. The activity of the Na^+-bound species is decreased to ~30% of the MVC-free state, NH_4^+ activates 5.7-fold, GP 2.2-fold, and the combination of Na^+ and GP (not shown) gives a 1.7-fold activation. The activity of the Na^+-bound αD56A species is only ~5% that of the Na^+-bound wild-type species, while the NH_4^+-bound αD56A species is activated 5-fold and exhibits an activity that is ~25% that of the NH_4^+-bound wild-type species. GP, and the combination of Na^+ and GP (not shown), also activate the mutant (by 2.2- and 1.7-fold, respectively), giving activities that are similar to those of the corresponding wild-type systems.

The effects of Na^+, K^+, and NH_4^+ on the $\alpha\beta$-reaction activities of the αD56A mutant are remarkably small in

comparison to the effects of these MVCs on the other mutants (Figure 3, panel B). Only NH_4^+ gives a slight activation (1.6-fold) over the MVC-free species, and, in comparison to the wild-type enzyme and the other mutants, this mutant exhibits the lowest set of $\alpha\beta$-reaction activities.

The binding of MVCs slightly decreases the α-reaction activities of the αD56A mutant in comparison to the rest of the MVC-free species (Figure 3, panel C). This behavior is similar to that of the wild-type enzyme and the other mutants. The α-reaction activity of the αD56A mutant is similar to that of the βK167T mutant, but significantly lower than the activities of the βD305N, βD305A, and wild-type systems.

The $\alpha\beta/\alpha$ activity ratio (Figure 4) for αD56A shows the α-site is only slightly activated by reaction of L-Ser at the β-site in the presence of Na^+ or K^+ (2- and 7-fold, respectively). Only NH_4^+ brings about significant activation (61-fold)

(d) βD305N. The β-reaction behavior of the βD305N mutant in the absence of MVCs is similar to the wild-type enzyme but exhibits activities that are lower by 2- to 6-fold for the Na^+ and K^+ species (Figure 3, panel A). In contrast to the behavior of wild-type enzyme, Na^+ has no stimulatory effects. K^+ only stimulates by 2-fold, whereas NH_4^+ stimulates the mutant enzyme by 6-fold. Inorganic phosphate alone or with Na^+ (data not shown) does not stimulate, and GP has an inhibitory effect (Figure 3, panel A).

In the absence of effectors, again, the mutant shows $\alpha\beta$-reaction activities somewhat similar to the wild-type enzyme (Figure 3, panel B). However, both Na^+ and K^+ weakly enhance the steady-state rates, whereas NH_4^+ stimulates 12-fold and brings the activity up to wild-type levels.

With the βD305N mutant, MVCs have essentially no effect on the α-reaction (Figure 3, panel C). Furthermore, the ratio of activities for the $\alpha\beta$- and α-reactions (Figure 4) shows that the α-reaction is only moderately activated by the
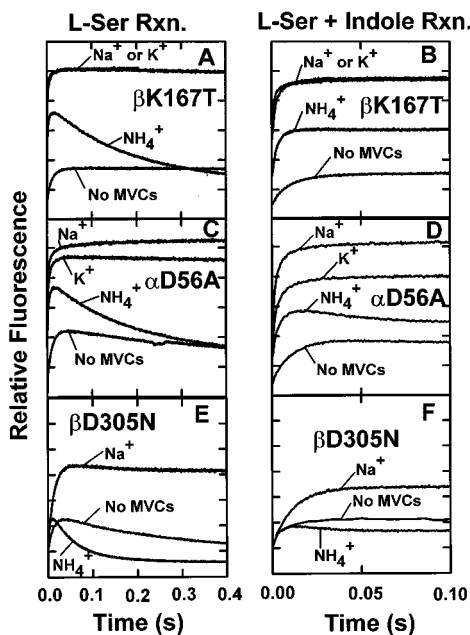
FIGURE 5: Fluorescence stopped-flow time courses are shown for the reactions of L-Ser, or L-Ser and indole with βK167T (A, B), αD56A (C, D), and βD305N (E, F). The reactions were carried out with the enzyme in one syringe, and 40 mM L-Ser (A, C), or 40 mM L-Ser and 1 mM indole (B, D) in the other syringe. Conditions: no monovalent cations, 100 mM NaCl, 10 mM KCl, and 50 mM NH_4Cl. Enzyme concentrations were 10 μM. All measurements were performed in pH 7.8 TEA buffer and 25.0 $\pm$ 2.0° C. The excitation wavelength was 425 nm, and fluorescence emission was measured at right angles to the excitation beam as a broad band through a window created by using the combination of a cutoff filter (below 430 nm) and Melles Groit glass filter BG23.

reaction of L-Ser at the β-site when Na^+ or K^+ are bound (11- and 9-fold, respectively), while the NH_4^+ species shows a 40-fold activation.

E(Aex1) Formation and Decay. (a) Fluorescence Stopped-Flow Measurements for Wild-Type Enzyme. To selectively follow the formation and decay of the E(Aex$_1$) species, fluorescence stopped-flow measurements were undertaken for the wild-type and mutant enzyme species (*14, 31*). Table 2 summarizes the effects of MVCs on these processes. Time courses for the mutant enzymes are given in Figure 5. The data for the wild-type enzyme (Table 2) establish that the relaxation rate constants for formation of E(Aex$_1$) are significantly increased by the binding of MVCs. In the absence of any MVC, E(Aex$_1$) formation is characterized by a relaxation of 200 s^{-1}; this value is increased to 900, 660, or 420 s^{-1} respectively, by Na^+, K^+, or NH_4^+. The Na^+ form of the enzyme exhibits two relaxations for the formation of E(Aex$_1$) with rates of 900 and 50$-$100 s^{-1} (*20*). Only a single relaxation for this process was detected for the K^+ and NH_4^+ forms. The rate behavior was found to be quite similar for E(Aex$_1$) formation and decay in the overall β-reaction.

(b) Fluorescence Stopped-Flow Measurements for βK167T. Figure 5, panels A and B, show representative time courses obtained both in the reaction of βK167T with L-Ser (A) and in the reaction of βK167T with L-Ser and indole (B). The relaxation rates for the different processes are summarized in Table 2. In the reaction of βK167T with L-Ser, Na^+, K^+, and NH_4^+ all stimulate E(Aex$_1$) formation (Figure 5, panel A, and Table 2), just as is seen with the wild-type enzyme

(Table 2). There is a detectable decay of E(Aex$_1$) only in the presence of NH_4^+. The reaction of the MVC-bound forms of βK167T with L-Ser and indole also show a stimulation of the fast phase that is similar to the behavior of the wild-type enzyme.

The pre-steady-state portion of the reaction of L-Ser and indole with βK167T (Figure 5, panel B) in the absence of MVCs, gives a time course showing that the steady-state level of E(Aex$_1$) is formed in a single phase (94 s^{-1}, Table 2) during a rapid pre-steady-state reaction. In the presence of NH_4^+, the pre-steady-state also is monophasic with the steady-state level of E(Aex$_1$) formed with a rate of 340 s^{-1} (Table 2). In the presence of Na^+ and K^+, E(Aex$_1$) is formed in a pre-steady-state that is biphasic (740 and 95 s^{-1}, and 522 and 97 s^{-1}, respectively).

(c) Fluorescence Stopped-Flow Measurements for αD56A. In both the reaction with L-Ser, and with L-Ser and indole, the kinetic behavior of αD56A (Figure 5, panels C and D) is very similar to that of the βK167T mutant (Figure 5, panels A and B, and Table 2). The E(Aex$_1$) formation rates in the presence of the MVCs are all very similar, with the Na^+ and K^+ complexes giving the fastest relaxations (360 and 600 s^{-1}, respectively). The NH_4^+ complex gives a rate of 250 s^{-1}, while the MVC-free species gives a rate of 94 s^{-1}. The NH_4^+ forms of the βK167T and αD56A mutants both show decay phases for conversion of E(Aex$_1$) to the E(A-A) intermediate (Figure 5, panels A and C), and the MVC-free αD56A species also exhibits a decay phase for this process (Figure 5, panel C).

The E(Aex$_1$) time courses for the reaction of L-Ser and Indole with the αD56A mutant (Figure 5, panel D) are similar to those observed in the reaction with L-Ser (Figure 5, panel C, and Table 2). Comparison with the βK167T reaction also shows a striking similarity.

Fluorescence Stopped-Flow Measurements for βD305N. In the reaction of βD305N with L-Ser (Figure 5, panel E, and Table 2), the fast phase of E(Aex$_1$) formation is slightly inhibited by Na^+(80 vs 100 s^{-1}) but is enhanced 2.5-fold by NH_4^+ (250 s^{-1}). In the absence of MVCs, the decay of the E(Aex$_1$) species is ~7-fold slower (3 s^{-1}) than was observed for the wild-type enzyme (21 s^{-1}) in the absence of effectors, and the value measured in the presence of Na^+ (6 s^{-1}) is the same as is seen with wild-type enzyme in the presence of Na^+ (Table 2). NH_4^+ ion stimulates this relaxation rate by ~6-fold over the MVC-free species.

In the pre-steady-state portion of the reaction of the mutant enzyme with L-Ser and indole (Figure 5, panel F, Table 2), again, there is no effect on the fast phase of E(Aex$_1$) formation by Na^+, whereas, NH_4^+ stimulates this process by 2.5-fold. The decreasing phase seen in the absence of effectors and in the presence of NH_4^+ has a very small amplitude. This relaxation is about 60-fold faster in the presence of NH_4^+.

Kinetic Isotope Effects and the Influence of Effectors on Activity. (a) Wild-Type Enzyme. Activity measurements for the β-reaction comparing isotopically normal L-Ser and α-^{2}H-L-Ser were performed to investigate the rate-limiting character of individual steps in the presence and in the absence of MVCs. The apparent KIE values from these measurements are summarized in Table 3. In the absence of MVCs and effectors, the wild-type enzyme exhibits a small KIE of 1.3. In the presence of Na^+ or K^+ (see refs *20* and *21*), substantial

Table 3: Influence of MVC Binding on Apparent Primary Kinetic Isotope Effects for the β-Reaction Activities of Wild-Type, βK167T, αD56A, and βD305N Mutant Enzymes with Isotopically Normal and α-^{2}H-L-Ser[a,b]

	primary KIE (k_H/k_D)			
MVC	βK167T	αD56A	βD305N	wild-type
none	2.7	7.6	2.8	1.3
Na$^+$	5.7	4.7	3.5	5.0
K$^+$	6.5	5.3		3.0
NH$_4$$^+$	6.8	3.7	2.8	1.2

[a] Rate measurements ($v_i/[E_O]$) were carried out as described in the legend to Figure 3. Conditions: [enzyme] = 0.5 μM; [serine derivative] = 40 mM; and when present, [NaCl] = 100 mM; [KCl] = 100 mM; [NH$_4$Cl] = 50 mM. [b] Error limits were estimated to be $\pm$ 5%.

KIE values were found (respectively, 5.0 and 3.0), whereas in the presence of NH$_4$$^+$, only a small KIE (1.2) is detected.

(b) *βK167T.* Apparent primary KIEs ranging from 2.7 to 6.8 are observed both with and without effectors in the βK167T system. The largest KIE was found in the presence of NH$_4$$^+$ (k_H/k_D = 6.8) (Table 3).

(c) *αD56A.* The β-reaction steady-state rates for the MVC-free, Na$^+$, K$^+$, and NH$_4$$^+$ forms of αD56A all exhibit large, apparent primary KIEs (7.6, 4.7, 5.3, and 3.7, respectively) (Table 3).

(d) *βD305N.* Apparent Primary KIEs were observed in the β-reaction catalyzed by βD305N both with, and without, MVCs. The magnitudes of the measured isotope effects (2.8 to 3.5) are similar both in the presence and in the absence of different effectors (Table 3).

Titration Studies with βK167T. Titration studies were performed to investigate NH$_4$$^+$ binding to the βK167T mutant enzyme. Two titrations were carried out: a static UV/Vis absorbance assay in which the dependence of the amplitude of the E(Q)$_{Indoline}$ absorption band on NH$_4$$^+$ ion concentration was used as a signal, and a titration of the β-reaction activity as a function of the NH$_4$$^+$ concentration. Both titrations gave data that were very well fit by the expression for the positive lobe of a rectangular hyperbola, indicating a single class of binding sites for NH$_4$$^+$. The apparent dissociation constant of 9.0 $\pm$ 0.3 mM obtained for the activity titration is about 4-fold higher than the value of 2.3 $\pm$ 0. 1 mM obtained for the quinonoid titration. Since the titration signals are coupled to different processes, the finding that these titration isotherms reflect significantly different hyperbolic constants is not unexpected.

DISCUSSION

The allosteric transitions for only a few protein systems are characterized both at atomic resolution and by detailed mechanistic studies (e.g., hemoglobin, aspartate transcarbamylase, the insulin hexamer, tryptophan synthase) (*4*, *6*, *7*, *16*, *17*, *26*, *38*−*40*). In each instance, transmission of the allosteric signal occurs via structural elements extending between sites and across the subunit interface. The relative free energies of different allosteric protein states are finely tuned so that ligand binding and/or covalent interactions trigger the allosteric transition. Use of site-directed mutagenesis to alter the protein scaffolding that transmits the allosteric signals can provide modified enzyme species well suited for examining the subtle relationship between structure and function.

This work examines the roles played both by the MVC site and by key amino acid residues in the transmission of allosteric signals between the α- and β-sites of the tryptophan synthase bienzyme complex. Cation substitutions at the MVC sites afford the equivalent of "inorganic" site-specific muta-tions. As is shown herein, the combination of MVC substitutions with the mutation of key amino acid residues makes possible a detailed analysis of events important to the transmission of allosteric signals in tryptophan synthase.

Structural Elements Involved in Allosteric Signaling. Three levels of conformational change comprise the allosteric transition in tryptophan synthase. These consist of domain motions in the β-subunit, loop motions in the α-subunit that close the α-site, and localized motions of residues extending between the β- and α-sites (*6*, *10*−*12*, *17*, *26*, *27*). The extent to which these conformational events are concerted during the $\alpha\beta$-catalytic cycle has not yet been established.[3]−The cycle of conformational events that occur during catalysis, as proposed by Pan et al. (*6*) and Woehl and Dunn (*20*, *21*) is shown in Scheme 2B.

In agreement with Scheme 2B, the results of X-ray crystallographic studies (*7*, *16*, *17*, *26*, *36*) (see Figure 1 and Table 1) show that the Na$^+$-, K$^+$-, and Cs$^+$-forms of wild-type E(Ain) crystallize with an open structure where loops 2 and 6 of the α-site are highly disordered, and where the β-site is accessible to solvent or L-Ser via a narrow entrance near the β−β subunit interface, as shown by the large magenta arrows in Figure 1, panels A and B (PDB files 1A5A; 1BKS; 1TTP; and 1TTQ; see Table 1 for references). Figure 1, panels A and B, complexes with ligands bound only to the α-site and with the β-site in the form of E(Ain) (*26*, *37*) give structures where loop 6 closes the α-site by folding down over the ligand (IPP or GP), making contacts with loop 2, and the β-site is open, or partially open (viz., PDB files 1A50, 1A5B, 1CW2) (Figure 1, panel B). The crystalline IPP and GP complexes of E(Aex$_1$) formed with the βK87T mutant give structures showing both the α- and the β-sites closed (Figure 1, panel C) (PDB files 2TRS and 2TSY, respectively). In these closed structures, two domains of the β-subunit have rotated relative to one another, blocking access to the β-site from solution (*17*). In the refined structure of the open conformation of the Na$^+$-complex of E(Ain) (PDB file 1BKS), both βK167 and βD305 appear to give two orientations, one with a βK167−βD305 salt bridge, the other with a βK167−αD56 salt bridge across the subunit

---

[3] The large body of evidence available concerning the linkage of conformational change to the allosteric transition between T- and R-states of the hemoglobin tetramer indicates local, tertiary, and global (quaternary) changes need not be concerted events (see for example, ref *40*). Crystallographic and solution studies have established that separate binding and/or covalent events at the α- and β-sites of tryptophan synthase can result in structures where either the α- or the β-sites reside in closed or partially closed conformations (*6*, *7*, *15*−*17*, *26*, *27*, *36*, *37*).

[4] The group I monovalent metal ions form complexes where the coordination geometry and coordination number are determined by steric and electronic constraints imposed by the ligand field and the charge density on the metal ion (*41*). Thus, while NH$_4$$^+$ is considered isosteric with K$^+$, there is no guarantee that NH$_4$$^+$ would give a complex at the Na$^+$/K$^+$/Cs$^+$ site of tryptophan synthase with a conformation identical to that of either the Na$^+$- or the K$^+$-complex. There are many examples of small molecule complexes where these three MVCs bind to the same site but give significantly different coordination structures (*41*).

interface (Figure 1, panel A). In the open conformations of the K^+- and Cs^+-complexes (PDB files 1TTQ and 1TTP), β-K167 forms a salt bridge across the subunit interface with αD56 (*16*), and the carboxylate of βD305 is solvent-exposed. With either IPP or GP bound, the Na^+-forms of the βK87T external aldimine of E(Aex$_1$) give closed conformations of both sites (Figure 1, panel C), as does the βK87T E(Aex$_2$) species (PDB file 2TYS), where βK167 forms the intersubunit salt bridge to αD56 (*17*). The switching of the βK167 side chain from the salt bridge with α-D56 to the salt bridge with β-D305 in the Na^+-form of E(Ain) (PDB file 1BKS) is accompanied by rearrangement of the βF280 and βY279 side chains. This rearrangement switches from a conformation where the tunnel is partially blocked, to a conformation where these residues form part of the tunnel wall (*16, 17*). In the absence of IPP or GP, the βK87T E(Aex$_1$) structure shows that the βD305 carboxylate makes an H-bond to the L-Ser β-hydroxyl of the E(Aex$_1$) (PDB file 1UBS). However, when either IPP or GP is bound, the βD305 carboxylate is too distant to form this H-bond, and, instead, forms a salt bridge to βR141 (Figure 1, panel C) (files 2TRS and 2TRY). The β-hydroxyl of E(Aex$_1$) (PDB files 1UBS, 2TRS, and 2TRY) and the indole moiety of E(Aex$_2$) (PDB file 2TYS) display different side-chain conformations: the hydroxyl is tilted forward, while the indole moiety is tilted back into the site and the ring N-H is H-bonded to the carboxylate of βE109 (*17*).

The mutations studied in this work were designed as probes for investigating both the structural linkages involved in the transmission of allosteric interactions between the α- and the β-sites (i.e., βK167, βD305, and αD56) and the potential involvement of βD305 in catalysis. The βD305 carboxylate may influence the chemistry of the β-site and the allosteric linkages between sites; both βK167 and αD56 are possible participants in the transmission of allosteric signals but are too remote from either site to be involved directly in catalysis (*17*). βD305 also is bonded via peptide links to two residues which make up part of the Na^+/K^+ site (βL304 and βF306).

Two MVC sites have been identified in tryptophan synthase. Na^+, K^+, and Cs^+ bind to a site (the $Na^+/K^+/Cs^+$ site) positioned about 8 Å from the phosphoryl group of PLP (Figure 1). Cs^+ also binds to a second site positioned on the β–β interface (the second Cs^+ site) (*16*). The ligand field geometry and coordination number at the $Na^+/K^+/Cs^+$ site depends on the bound MVC. Na^+ and K^+ coordinate to the carbonyl oxygens of Phe-306, Ser-308, and Gly-232, and the inner coordination spheres of these complexes also include water (one for K^+, and two for Na^+). The Cs^+ ligand field includes three additional backbone carbonyl oxygens (Val-231, Gly-268, and Leu-304) but no water molecules (*16*).

The refined structure of the Na^+-form of E(Ain) (PDB file 1BKS) implies that βLys167 can switch back and forth between the alternative salt bridges with αD56 and βD305 (Figure 1, panel A). If this occurs as $\alpha\beta$-subunit pairs undergo conformational transitions between open, partially closed, and closed structures during the catalytic cycle (*6*), then the switch between these alternative salt bridges could be part of the protein scaffolding involved in the transmission of allosteric signals between the α- and β-sites. The α-sites of E(Ain), E(GD$_1$), E(GD$_2$), E(Aex$_1$) and E(Aex$_2$) reside in

low activity states, whereas, the α-sites of E(A-A) and E(Q$_3$) reside in high activity states, and the switch between open or partially closed states to the closed states of the $\alpha\beta$ dimeric unit appears linked to the changes in α-site activity (*6, 12, 13, 20, 21*).

Prior work (*15–21, 25–27*) shows that the MVC-bound forms of the wild-type E(A-A), E(Q$_3$), and E(Q)$_{Indoline}$ species represent closed conformation states of the β-subunit (Table 1) that trigger activation of the α-site for reaction when IGP binds, whereas the MVC-free species do not (*12–15*). The MVC-bound forms of the E(Ain)(L-Ser) Michaelis complex and E(Aex$_1$) represent open and partially closed β-subunit states, respectively, wherein the α-site is deactivated (*12*). As will be shown, either MVC removal, or mutations at certain loci disrupt the triggering of α-site activation, and this disruption can be partially or fully repaired by MVC binding, ligand binding to the α-site, or increased temperature (*15–21, 25–27*).

The data presented in Figures 2–5 and summarized in Table 4 document a range of effects due to mutation and/or MVC substitution on the distribution of intermediates and the kinetic behavior of tryptophan synthase. Significant effects arise where the mutation and/or MVC substitution strongly influences either the ability of the β-site to form one or another of the intermediates, or the transmission of the allosteric signal that triggers activation of the α-site (see Table 4).

Comparisons of Wild-Type, βK167T, αD56A, and βD305N Tryptophan Synthases. (a) The MVC-Free Species. The MVC-free βK167T and αD56A mutants exhibit striking differences in behavior from the wild-type enzyme and the βD305N mutant with respect to the distribution of intermediates at equilibrium for reactions at the β-site (compare Figure 2, panels A–H and Tables 1 and 4) (*14, 19–21*). In stage I of the β-reaction, the MVC-free wild-type and βD305N mutant species give distributions of intermediates strongly shifted in favor of E(A-A) with only small amounts of E(Aex$_1$) present and with little or no substrate Michaelis complex (Figure 2, panels A and G, and Tables 1 and 4). However, the MVC-free wild-type E(A-A) species does not have an activated α-site, and the MVC-free E(A-A) of βD305N shows only a small degree of activation (Figure 4, Table 4). Both βK167T and αD56A give mixtures dominated by E(Aex$_1$) with smaller amounts of the E(Ain) species in a Michaelis complex with L-Ser. No more than a trace of E(A-A) is present in the equilibrating mixtures obtained for the βK167T and αD56A systems (Figure 2, panels C and E, and Figure 5). The βK167T system shows some activation of the α-site, while αD56A does not. It may be that IGP binding shifts the distributions of β-site species for both βK167T and βD305N, thereby increasing the fraction of sites in the E(A-A) state, just as GP binding shifts these systems to the E(A-A) state (Figure 2; Table 4), and this shift partially restores the activation linkage.

In the reaction of L-Ser with the indole analogue, indoline (Figure 2), only very small amounts of E(Q)$_{Indoline}$ are formed for the wild-type or mutant enzymes in the absence of MVCs. However, both wild-type enzyme and the βD305N mutant give more E(Q)$_{Indoline}$ than either βK167T or αD56A. Although the MVC-free wild-type and βD305N species show preferential stabilization of E(A-A), E(Q)$_{Indoline}$ formation from these MVC-free E(A-A) species is significantly im-

Table 4: Comparison of the Effects of Mutation and Effector Binding on the Properties of the Wild-Type (WT), βK167T, αD56A, and βD305N Mutant Tryptophan Synthase Derivatives

enzyme	MVC/ effector[a]	major species; UV/Vis spectra[b] (see Figure 2)		steady-state activities[c] (see Figures 3 and 4)				transient kinetics, L-Ser reaction (see Figure 5 and Table 2)		C-α scission RDS[f] (Table 3)
		L-Ser Rxn.	L-Ser + indoline Rxn.	β-Rxn.	α-Rxn.	$\alpha\beta$-Rxn.	α-activation $\alpha\beta/\alpha$	E(Aex$_1$) form[d]	E(Aex$_1$) decay[e]	
WT	none	E(A-A)	E(A-A)	suppressed	normal	suppressed	deactivated	medium	yes (fast)	no
	Na$^+$	E(Aex$_1$) + E(A-A)	E(Q)$_{Indoline}$	normal	normal	normal	activated	fast	yes (fast)	yes
	K$^+$			normal	normal	normal	activated	fast	yes (fast)	
	NH$_4^+$	E(A-A)	E(A-A)	normal	normal	normal	activated	medium	yes (fast)	no
	GP	E(A-A)	E(A-A)	suppressed						
	Na$^+$ + GP	E(A-A)	E(Q)$_{Indoline}$							
βK167T	no MVC	E(Ain) + E(Aex$_1$)	E(Ain) + E(Aex$_1$)	defective	WT-like	defective	deactivated	slow	no	yes
	Na$^+$	E(Aex$_1$)	E(Aex$_1$)	defective	WT-like	partially repaired	activated	fast	no	yes
	K$^+$			defective	WT-like	partially repaired	activated, WT-like	fast	no	yes
	NH$_4^+$	E(A-A)	E(Aex$_1$) + E(Q)$_{Indoline}$	partially repaired	WT-like	repaired	activated, WT-like	medium.	yes (slow)	yes
	GP	E(A-A)	E(Aex$_1$) + E(Q)$_{Indoline}$	suppressed						
	Na$^+$ + GP	E(Aex$_1$) + E(A-A)	E(Q)$_{Indoline}$							
αD56A	no MVC	E(Ain) + E(Aex$_1$)	E(Ain) + E(Aex$_1$)	defective	WT-like	defective	deactivated	slow	yes (slow)	yes
	Na$^+$	E(Aex$_1$)	E(Aex$_1$)	defective	defective	defective	deactivated	medium	no	yes
	K$^+$				defective	defective	partially activated	fast	no	yes
	NH$_4^+$	E(Aex$_1$) + E(A-A)	E(Aex$_1$) + E(A-A)	partially repaired	defective	partially repaired	activated, WT-like	medium	yes (slow)	yes
	GP	E(Aex$_1$) + E(A-A)	E(Aex$_1$) + E(A-A)	suppressed						
	Na$^+$ + GP	E(Aex$_1$) + E(A-A)	E(Q)$_{Indoline}$							
βD305N	no MVC	E(A-A)	E(A-A)	suppressed	WT-like	defective	deactivated	slow	yes (slow)	yes
	Na$^+$	E(Aex$_1$)	E(Q)$_{Indoline}$	partially repaired	WT-like	partially repaired	activated	slow	yes (slow)	yes
	K$^+$			partially repaired	WT-like	partially repaired	partially activated			
	NH$_4^+$	E(A-A)	E(Q)$_{Indoline}$	WT-like	WT-like	WT-like	activated, WT-like	medium	yes (fast)	yes
	GP	E(A-A)	E(A-A)	suppressed						
	Na$^+$ + GP	E(A-A)	E(Q)$_{Indoline}$							

[a] When present, effector concentrations were as follows: 100 mM NaCl, 100 mM KCl, 50 mM NH$_4$Cl, 50 mM MVC-free GP, or 200 mM NaCl + 50 mM GP. [b] The major species present was determined by inspection of Figure 2. Where there appears to be comparable amounts of more than one species, all are listed. [c] Analysis based on Figures 3 and 4. The terminology used reflects the following activity relationships: "normal", the activities of MCV-activated wild-type enzyme; "suppressed", the activity of MVC-free wild-type enzyme; "defective", a mutant activity level that is significantly lower than that of the corresponding wild-type enzyme system; "WT-like", a mutant activity that has been restored to a wild-type like level; "partially repaired", a mutant activity that has been partially restored to a wild-type like level; "repaired", a mutant activity that has been restored to a significantly higher level, but does not achieve a wild-type like value. [d] Analysis based on Table 3. The designations, slow (<100 s^{-1}), medium ($\sim$100 to 350 s^{-1}), and fast (>350 s^{-1}) refer to the rate of the faster relaxation for the appearance of E(Aex$_1$). [e] The designations "yes" or "no" refer to the observation of a relaxation for the conversion of E(Aex$_1$) to E(A-A). The designations "slow" (<10 s^{-1}) and "fast" (>10 s^{-1}) refer to the rate of the faster relaxation for the conversion of E(Aex$_1$) to E(A-A). [f] As judged by a KIE > 2.0 (k_H/k_D), proton abstraction from the C-α of E(Aex$_1$) is assigned as the dominating, rate-determining step (RDS) for substrate turnover in the β-reaction.

paired (Figure 2, Table 4). The MVC-free βK167T and αD56A species preferentially stabilize E(Aex$_1$) and react with difficulty to form E(A-A) and E(Q)$_{Indoline}$, indicating that the closed conformations of E(A-A) and E(Q)$_{Indoline}$ have been destabilized.

Turnover rates measured for the β-reaction (Figure 3, panel A) in the absence of MVCs show large disparities in activities. The catalytic cycle of the β-site is greatly impaired by the replacement of βLys167 by Thr, while the β-activities of the MVC-free wild-type, αD56A, and βD305N species are similar. Nevertheless, the wild-type and mutant enzymes

in the absence of MVCs all give $\alpha\beta$-reaction turnover rates that are essentially identical (Figure 3, panel B; Table 4), indicating that IGP binding to the α-site partially restores β-site activity for βK167T. The α-reaction of βK167T is 14-fold slower than that of wild-type enzyme, while βD305N is 4-fold slower and αD56A is 10-fold slower (Figure 3, panel C).

The formation of E(Aex$_1$) with the βK167T, αD56A, and βD305N mutants exhibit rates similar to the MVC-free wild-type enzyme (viz. Figure 5, and Table 2). No transient decay of E(Aex$_1$) to E(A-A) occurs with the βK167T and αD56A

mutants. The βD305N mutant shows a decay phase but with a rate that is 7-fold slower than wild-type enzyme. Clearly, these mutations have little effect on the steps leading to E(Aex$_1$) formation, but α-proton abstraction from E(Aex$_1$) and/or the transition to the closed conformation of E(A-A) is impaired. Similar behavior is seen in the pre-steady-state time courses of the $\alpha\beta$-reaction (Figure 5 and Table 2).

In the β-reaction, the MVC-free βK167T, αD56A, and βD305N mutants show apparent primary KIEs of 2.7, 7.6, and 2.8, respectively, in the steady-state for removal of the E(Aex$_1$) α-proton, while the wild-type enzyme shows almost no effect (KIE = 1.3) (Table 3). Thus, this process is at least partially rate determining for the mutants but not for the wild-type enzyme.

The behaviors of the MVC-free βD305N mutant and the MVC-free wild-type enzyme are very similar but not identical (Figures 2−5), indicating the mutant retains most of the functional capabilities of the wild-type system. Therefore, the negative charge of the βD305 carboxylate does not play a critical role in catalysis, and the amide of the Asn side chain is able to substitute for any functional role(s) played by βAsp305. Clearly, any such functional roles do not strongly depend on the negative charge of the carboxylate.

The behavior of the MVC-free βK167T and αD56A mutants strongly diverge from that of the wild-type and βD305N species with respect to the distribution of intermediates in stage I (Figure 2). This divergence implies that both βK167 and αD56 play critically important roles in linking conformational events to chemical events in the functioning of the bienzyme complex.

The available structural data implicate a salt bridging role for βK167 and αD56A (16) in the transmission of allosteric signals between the sites. The altered properties of βK167T and αD56A most likely have their origins in destruction of the salt bridge formed between βK167 and αD56. Since the distribution of intermediates in stage I is largely unaffected by the βD305N mutation, and since this mutant exhibits behavior similar to the wild-type enzyme, it is likely that the predominating effect stems from the inability of the βK167T and αD56A mutants to form the βK167 to αD56 salt bridge across the $\alpha-\beta$ subunit interface rather than a strongly perturbed interaction involving either the βK167−βD305 salt bridge or the βD305−βR141 salt bridge. The functional role of a salt-bridge between βK167 and βD305 is less clear. βD305N very likely is capable of forming the conformation associated with these salt bridges via H-bonding of the side chain amide of Asn to the ϵ-ammonium of βLys 167 or to the guanidinium of βR141 (even though the charge−charge interaction is lost).

The finding that MVC-free βK167T shows a strongly impaired β-reaction activity when compared to αD56A, β305N, and wild-type enzyme is a striking result (Figure 3, panel A). This is seen again in the Na$^+$ and K$^+$ systems (see below) and strongly implies that the βK167T mutant is unable to undergo facile switching between the two conformation states associated with the salt bridges to βD305 and αD56. Consequently, the distribution of open and closed conformations appears to be more strongly altered than for the other two mutants, and catalysis is more strongly impaired.

(b) The Na$^+$ Activated Species. The Na$^+$, K$^+$, Cs$^+$, and NH$_4^+$ complexes of the wild-type system give catalytically and allosterically functional enzymes with similar, but not identical, properties (14, 18−21). As demonstrated by Peracchi et al. (19) and by Woehl and Dunn (14, 20, 21), the MVC-bound forms of the wild-type enzyme persist in activated states relative to that of the MVC-free enzyme (Figures 3 and 4). Furthermore, the allosteric communication between sites is impaired in the MVC-free species (14). As compared to the MVC-free enzyme, Na$^+$ binding to the wild-type system causes a redistribution of intermediates formed in the L-Ser reaction, giving an equilibrium where the proportions of the E(Aex$_1$) and E(A-A) species are comparable and other species are minor (14, 20, 21) (see Figure 2, panel A).

In the L-Ser reaction, Na$^+$ binding favors E(Aex$_1$) slightly more than E(A-A) (compare Figure 2, panels A and G). The reactions of the Na$^+$ forms of the βK167T and αD56A mutants with L-Ser (Figure 2 panels C and E, and Figure 5, panel A, and C) are quite different from the wild-type enzyme; these mutations strongly stabilize E(Aex$_1$) with almost complete exclusion of other species. The K$^+$ forms behave similarly. The divergence from wild-type-like behavior is again indicated by the difficulty with which the Na$^+$ complexes of βK167T and αD56A form E(A-A) or E(Q)$_{Indoline}$ (Figure 2). This finding is further supported by rapid-scanning stopped-flow kinetic experiments (data not shown) that failed to detect quinonoidal species either in the pre-steady-state or the steady-state of the β-reaction of the βK167T mutant.

The Na$^+$ and K$^+$ forms of βD305N show some impairment of the β- and $\alpha\beta$-reactions, and there is some impairment of the activation of the α-site (see Figures 3 and 5, and Table 4). The formation of E(Aex$_1$) in stage I of the L-Ser reaction is significantly slowed in the mutant ($1/\tau_1 = 80$ s^{-1} for βD305N, vs 900 s^{-1} for wild-type enzyme) (Table 2). The pre-steady-state phase of the β-reaction also is similarly diminished. Interestingly, the βK167T mutant shows an E(Aex$_1$) formation rate that is comparable to wild-type enzyme (750 vs 900 s^{-1}), and the αD56A mutant gives a formation rate of 360 s^{-1} (Figure 5 and Table 2), indicating that the βK167−αD56 salt bridge has little affect on formation of the L-Ser aldimine.

The finding that the Na$^+$ form of βD305N shows an impaired rate of E(Aex$_1$) formation is consistent with the suggestion that in wild-type enzyme, βD305 assists formation of this species through H-bonding with the β-hydroxyl of the reacting substrate (17), and that mutation to Asn interferes with this assistance. The X-ray structures of β-site intermediates indicate that the carboxylate of βD305 is also important for the stabilization of the closed conformation through formation of a H-bonded salt bridge with βR141. Apparently, the neutral amide group can replace the carboxylate in this H-bonding interaction and the negative charge is relatively unimportant. Consequently, the near wild-type-like behavior of the βD305N mutant otherwise implies that the replacement of the Asp carboxylate by an amide group represents a relatively minor perturbation of the functional properties of the β-site.

Steady-state turnover rates for the Na$^+$-activated enzymes (Figure 3) show that for the β-reaction, wild-type enzyme is 82-fold more active than βK167T, 37-fold more active than

αD56A, and 4-fold more active than βD305N. In contrast, the α- reaction (Figure 3, panel C) shows little variation in activity (3- to 10-fold) between wild-type and mutant enzymes. The $\alpha\beta$ reaction (Figure 3, panel B) is more strongly influenced by the mutations: wild-type enzyme is 10-fold more active than βK167T, 107-fold more active than αD56A, but only 4-fold more active than βD305N.

The effects of ^{2}H substitution for ^{1}H at the Ser C-α (Table 3) show large observed primary KIEs on β-reaction turnover rates in the presence of Na$^+$, both for the wild-type enzyme (5.0) and for βK167T (5.7), and αD56A (4.7) (Table 3). Except for αD56A, these KIEs are considerably increased over the values obtained for the MVC-free species.

These comparisons indicate that the altered kinetic and thermodynamic properties brought about by the βK167T and αD56A mutations are not repaired by the binding of Na$^+$. Indeed, some of the differences between wild-type enzyme and the βK167T, βD305N, and αD56A mutants are accentuated in the Na$^+$ complexes. The strong stabilization of E(Aex$_1$) by the Na$^+$ forms of βK167T and αD56A, and the inability of the Na$^+$ forms of these mutants to stabilize E(Q)$_{Indoline}$ are remarkable. One consequence of these three mutations is to favor the partially closed conformation of the Na$^+$-bound E(Aex$_1$) species and minimize the closed conformation of the E(A-A) species (*15*, *20*, *21*). Consequently, only the βK167T system shows significant activation of the α-site in the reaction with L-Ser. Since the rate of E(Aex$_1$) formation with the βK167T mutant is very similar to that of the wild-type system, and the αD56A mutant is slowed by only a factor of 2 to 3 (Table 2), it is evident that the chemical and conformational events preceding E(Aex$_1$) formation are essentially unperturbed by the Lys to Thr mutation at β167 and only slightly perturbed by the Asp to Ala mutation at α56. Therefore, impairment of catalysis (Figure 3, panels A and B) must occur in the process of converting E(Aex$_1$) to E(A-A), a transformation dependent on formation of the closed conformation (*15*, *20*, *21*).

(c) The NH$_4^+$ Activated Species. The effects of NH$_4^+$ both on the static spectra obtained in the L-Ser reaction and on the formation of E(Q)$_{Indoline}$ (Figure 2) establish that the NH$_4^+$ species all exhibit properties that are significantly altered in comparison to the MVC-free, Na$^+$ and K$^+$ species. In the L-Ser reaction, the NH$_4^+$-substituted wild-type and βD305N mutant enzymes give distributions of E(Aex$_1$) and E(A-A) that fall between the extremes represented by the MVC-free systems and the Na$^+$-activated systems. The NH$_4^+$ form of the βK167T mutant stabilizes the E(A-A) species to a greater extent than does either the metal-free or the Na$^+$-bound systems. The relative amounts of E(Aex$_1$) and E(A-A) formed at equilibrium in the presence of NH$_4^+$ appear nearly identical for wild-type enzyme and for the βK167T and βD305N mutants. The αD56A mutant gives a mixture with less E(A-A). The E(Aex$_1$) fluorescence time courses (Figure 5, Table 2) for the NH$_4^+$-forms of the wild-type and βK167T mutant enzymes are remarkably similar.

NH$_4^+$ is reasonably effective in stabilizing E(Q)$_{Indoline}$ for all of the enzyme species. The behaviors of the NH$_4^+$-substituted βK167T and αD56A systems are in marked contrast to that of the Na$^+$ systems, where no detectable amount of E(Q)$_{Indoline}$ accumulates. Ammonium ion strongly stabilizes the βD305N quinonoid, less strongly stabilizes the wild-type and βK167T quinonoids, and gives little or no

stabilization to the αD56A quinonoid (Figure 2). Figures 2, 3, and 5 establish that NH$_4^+$ binding gives very similar wild-type and mutant enzyme species wherein the interconversion of the open and closed states is facile.

The steady-state kinetic studies presented in Figures 3 and 4 show that, of the MVCs studied in this work, NH$_4^+$ is the most effective cation for activating the β-reactions of the wild-type and all three mutant enzymes. NH$_4^+$ is highly effective also in stimulating the $\alpha\beta$-reactions of the wild-type, βK167T, and βD305N enzymes and in activating the α-site in the $\alpha\beta$-reaction. Only Cs$^+$ (*18*, *19*) is more effective than NH$_4^+$ in stimulating the β and $\alpha\beta$ reactions. Like the other MVCs, NH$_4^+$ has little or no effect on the α-reaction (Figure 3, panel C). The large apparent KIEs found in the L-Ser reaction (Table 3) establish that abstraction of the α-proton from E(Aex$_1$) dominates the rate-limiting process for turnover of the βK167T mutant, whereas, the smaller KIEs observed for the βD305N and wild-type systems indicate other steps dominate.

The NH$_4^+$-substituted wild-type, βK167T, αD56A, and βD305N enzyme systems all show comparable β-reaction turnover rates (within a factor of $\sim$3; Figure 3), and all but αD56A show comparable $\alpha\beta$-reaction turnover rates. All are able to form equilibrating mixtures of E(Aex$_1$) and E(A-A) in the reaction with L-Ser, and substantial amounts of E(Q)$_{Indoline}$ accumulate in the indoline reaction for all four enzyme species (Figure 2). These signatures of structure$-$function imply that NH$_4^+$ provides significant repair of the defects introduced by the mutations. The substitution of NH$_4^+$ into the MVC sites of the wild-type and βD305N mutant enzymes gives species with properties that are not unlike those of the Na$^+$ and K$^+$ substituted species. Nevertheless, only NH$_4^+$ restores βK167T and αD56A to wild-type-like states, especially with full allosteric communication between the α- and β-sites (see Figure 4). Therefore, we conclude that there is something different about the interactions of NH$_4^+$ with βK167T and αD56A that is not replicated by the interactions of Na$^+$ or K$^+$ with these mutants.

We consider it highly likely that NH$_4^+$ binds to the Na$^+$/K$^+$/Cs$^+$ site adjacent to the β-catalytic site. Additionally, there is a second possible locus for NH$_4^+$ binding that is common to wild-type enzyme and all the mutants, the second Cs$^+$ site located at the $\beta-\beta$ subunit interface. Cs$^+$ is the only MVC that has been shown to bind in this site (*16*). The ionic radius of Cs$^+$ (1.69 Å) is significantly larger than Na$^+$ (0.95 Å) and K$^+$ (1.33 Å) but not too different from NH$_4^+$ (1.49 Å). The structural and kinetic effects (if any) of MVC binding to the second Cs$^+$ site are not well understood. This site does not bind Na$^+$ or K$^+$ sufficiently tightly to give complexes identifiable by X-ray diffraction (*16*).

Nevertheless, since our binding studies indicate a single class of noninteracting sites for NH$_4^+$, restoration of wild-type-like properties by NH$_4^+$ appears to result from binding to a single site, and that site probably is the Na$^+$/K$^+$/Cs$^+$ site. In contrast to the complexes formed with other MVCs, the NH$_4^+$ complex is restricted to a tetrahedral, or distorted tetrahedral, geometry dictated by H-bonding of the four N-H protons to acceptor ligands from the protein or water (*41*). Therefore, we conclude that the effectiveness of NH$_4^+$ in rescuing the mutants is due to the different bonding requirements of NH$_4^+$, which restore wild-type-like conformational stabilities and dynamics to the mutants.

Interactions between the α-Site, the MVC Site, and the β-Catalytic Site. (a) The GP Effect in the Absence and Presence of Na$^+$. GP binds to a single site, the α-catalytic site (*17*). Like G3P (*12*), GP in the presence of MVCs, is a potent allosteric effector of the distribution of intermediates in the reaction of L-Ser with PLP at the β-site 25 Å away (*5, 6, 10–12, 15, 22, 42, 43*). Nevertheless, in the absence of MVCs, the binding of GP has only minor effects both on the distribution of intermediates formed in the reaction of wild-type enzyme with L-Ser, and on the reaction of L-Ser and indoline (compare the MVC-free spectra with the spectra measured in the presence of GP, Na$^+$ and the combination of Na$^+$ and GP, Figure 2) (*14*). This finding emphasizes the essential allosteric role played by MVCs in site–site communication.

The binding of GP has similar effects on both the βD305N mutant and the wild-type enzyme (Figure 2). However, the βK167T and αD56A mutants show interesting differences from the behavior of the wild-type and βD305N systems. The most striking effect arises from the synergism between MVC binding and GP binding. In the presence of Na$^+$, the binding of GP to the wild-type and βD305N mutant enzymes strongly favors E(A-A) in the L-Ser reaction, and this combination provides the strongest stabilization of the quinonoidal species in the reaction with L-Ser and indoline (Figure 2, panels B and H). In contrast, the Na$^+$-substituted βK167T and αD56A systems both stabilize E(Aex$_1$) in the L-Ser reaction, while GP binding partially reverses the effects of Na$^+$ alone, giving comparable amounts of E(Aex$_1$) and E(A-A). In the reaction of L-Ser and indoline, neither mutant gives a detectable amount of quinonoid in the presence of Na$^+$, whereas the combination of GP and Na$^+$ provides the greatest stabilization of E(Q)$_{Indoline}$.

We propose that the impaired properties of these mutants arise from a shift in the distribution of enzyme states to an ensemble where the catalytically active forms are relatively rare species. Restoration of function by the combined actions of Na$^+$ and GP then is a consequence of the ligand-mediated shift of the mutants to a conformational ensemble similar to that of the wild-type enzyme. The allosteric (synergistic) effects of Na$^+$ and GP act to overcome the adverse effects of the mutations on the distribution of enzyme forms. The combination of GP and Na$^+$ binding drives the α- and β-subunits to closed conformations as L-Ser is converted to E(A-A) and then to E(Q)$_{Indoline}$.

(b) Differences Between the αD56A and βK167T Mutants. As judged by several of the criteria applied in this study, the αD56A and βK167T mutations elicit remarkably similar effects on many of the catalytic and regulatory properties of tryptophan synthase (viz. Figures 2–5). However, there are also interesting differences. For example, MVC-free αD56A exhibits a significantly higher β-reaction activity, αD56A is less responsive to activation by Na$^+$, K$^+$, and NH$_4^+$ in the αβ-reaction, and αD56A is less responsive to activation of the α-reaction by Na$^+$ and K$^+$ (Figures 3 and 4). These differences can be rationalized in the following way. According to the salt-bridging hypothesis, βK167 must interact both with αD56 and βD305, i.e., these carboxylates compete for βK167. It then follows that the mutation of αD56 to L-Ala should destabilize conformations that correspond to salt-bridging between βK167 and αD56 in the wild-type enzyme and bias the system toward alternative conformations,

including the salt bridge to βD305. Since the side chain of βThr 167 in βK167T is unable to form salt bridges to either αD56 or βD305, this mutation likely alters the distribution of conformation states differently from that of the αD56A mutation. Therefore, it is reasonable to expect that the αD56A and βK167T mutations exert different effects on the conformational ensemble, and, therefore, it is not surprising that some details of the catalytic and regulatory behavior of these two mutants are different.

(c) Activation of the α-Site via L-Ser Reaction at the β-Site. The activation of the α-site in response to the conversion of E(Aex$_1$) to E(A-A) is a critically important allosteric function of the reaction of L-Ser in stage I of the β-reaction during the αβ-reaction that serves to couple the catalytic cycles of the α- and β-sites (*6, 8–13*). This allosteric effect is impaired in the MVC-free wild-type and mutant enzymes (Figure 4). Significant activation is obtained in the Na$^+$ (30-fold), K$^+$ (26-fold) and NH$_4^+$ (40-fold) forms of the wild-type enzyme. The Na$^+$ forms of the βK167T and βD305N mutants also show significant activation (12- and 11-fold, respectively), while the αD56A mutant is only slightly activated (2-fold). The K$^+$ forms of βK167T, βD305N, and αD56A are activated 46-, 9-, and 7-fold, respectively. All of the mutants are strongly activated by NH$_4^+$: βK167T by 34-fold, αD56A by 61-fold, and βD305N by 40-fold. This allosteric signal triggers both the activation of the α-site and the switch to a closed structure (*6, 9, 12, 13*). Therefore, the extent of activation in each instance roughly parallels the extent to which the distribution of species formed in stage I of the L-Ser reaction favors the formation of E(A-A) (viz., Figures 2 and 4).

Implications for Enzyme Catalysis. In previous works, we have demonstrated that conformation change is an integral and important component of the catalytic cycle of the tryptophan synthase bienzyme complex (*5, 10–15, 18, 20, 21, 31, 32, 41, 43*). There are at least three functions associated with the cycle of conformational changes that occur during catalysis. One function involves the switching of αβ-subunit pairs between open and partially closed conformations to closed conformations as a means for regulating access of substrates and products in to and out of the complex, and, most importantly, to achieve efficiency in the channeling of indole between the α- and β-sites (see Scheme 2B) (*6, 15*). The second function is to couple the α- and β-reactions by switching the α-site on and off in response to covalent transformations at the β-site. The third is to facilitate the chemical steps at the α- and β-sites via a set of conformational transitions that provide complementarity between the site and the reacting substrate for each transition state along the reaction pathway (*5, 10–15, 20, 21, 31, 32, 41*). In the tryptophan synthase system, our studies have revealed two important functions for the Na$^+$/K$^+$/Cs$^+$ MVC site: (a) modulation of the interconversion between the open, partially closed and closed conformation states of the αβ-dimeric unit (*6, 10, 11, 14, 15, 20, 21*), and (b) modulation of the strength of bonding interactions between the protein and the intermediates and activated complexes along the reaction path (*14, 20, 21*).

These experiments establish that effector binding to the mutant enzymes at either of two quite distinctly different loci (i.e., the Na$^+$/K$^+$/Cs$^+$ site on the β-subunit, or the α-catalytic site) can restore (a) wild-type like-states of

catalytic activity, and (b) wild-type-like distributions of covalent intermediates at the β-site. It is striking that, of the effectors examined in this study, the β-reaction activity of the αD56A mutant is restored to a wild-type-like behavior by only one effector (e.g., NH_4^+, see Figures 3 and 5). Other studies (*19, 24, 25*) show that Cs^+ is even more effective in restoring wild-type behavior. Repair by NH_4^+ is in accord with the finding that this ion gives distributions of species for the mutant systems that are similar to wild-type enzyme (Figure 2). In contrast to the behavior of NH_4^+, the strong effects of the βK167T and αD56A mutations on the α- and $\alpha\beta$-reactions are not repaired by Na^+ or K^+ binding. We postulate that the repair of function by NH_4^+ involves alteration of the protein conformational dynamics to re-establish wild-type-like relative free energies for the distribution of intermediates and for activation energies along the reaction path that restores wild-type-like functions. Owing to differences in coordination geometry, and/or the binding loci, NH_4^+ is much more effective than either Na^+ or K^+ in bringing about this redistribution.

REFERENCES

1. Yanofsky, C., and Crawford, I. P. (1972) in *The Enzymes*, 3rd ed. (Boyer, P. D., Ed.), pp 1−31, Academic Press, New York.
2. Miles, E. W. (1979) *Adv. Enzymol. Relat. Areas Mol. Biol. 49*, 127−186.
3. Miles, E. W. (1995) In *Subcellular Biochemistry, Vol 24*: *Proteins: Structure, Function and Protein Engineering* (Biswas, B. B., and Roy, S. eds) pp 207−254, Plenum Press, New York.
4. Miles, E. W., Rhee, S., and Davies, D. R. (1999) *J. Biol. Chem. 274*, 12193−12196.
5. Dunn, M. F., Aguilar, V., Brzovic, P. S., Drewe, W. F., Jr., Houben, K. F., Leja, C. A., and Roy, M. (1990) *Biochemistry 29*, 8598−8607.
6. Pan, P., Woehl, E., and Dunn, M. F.(1997) *Trends Biochem. Sci. 22*, 22−27.
7. Hyde, C. C., Ahmed, S. A., Padlan, E. A., Miles, E. W., and Davies, D. R. (1988) *J. Biol. Chem. 263*, 17857−17871.
8. Lane, A. N., and Kirschner, K. (1991) *Biochemistry 30*, 479−484.
9. Anderson, K. S., Miles, E. W., and Johnson, K. A. (1991) *J. Biol. Chem. 266*, 8020−8033.
10. Brzovic, P. S., Sawa, Y., Hyde, C. C., Miles, E. W., and Dunn, M. F. (1992) *J. Biol. Chem. 267*, 13028−13038.
11. Brzovic, P. S., Hyde, C. C., Miles, E. W., and Dunn, M. F. (1993) *Biochemistry 32*, 10404−10413.
12. Brzovic, P. S., Ngo, K., and Dunn, M. F. (1992) *Biochemistry 31*, 3831−3839.
13. Leja, C. A., Woehl, E. U., and Dunn, M. F. (1995) *Biochemistry 34*, 6552−6561.
14. Woehl, E. U., and Dunn, M. F. (1995) *Biochemistry, 34*, 9466−9476.
15. Pan, P., and Dunn, M. F. (1996) *Biochemistry 35*, 5002−5013.
16. Rhee, S., Parris, K. D., Ahmed, S. A., Miles, E. W., and Davies, D. R. (1996) *Biochemistry 35*, 4211−4221.
17. Rhee, S., Parris, K. D., Hyde, C. C., Ahmed, S. A., Miles, E. W., and Davies, D. R. (1997) *Biochemistry 36*, 7664−7680.
18. Fan, Y.-X., McPhie, P., and Miles, E. W. (2000) *Biochemistry 39*, 4692−4703.
19. Peracchi, A., Mozzarelli, A., Rossi, G. L. (1995) *Biochemistry 34*, 9459−9465.
20. Woehl, E. U., and Dunn, M. F. (1999) *Biochemistry 38*, 7118−7130.
21. Woehl, E. U., and Dunn, M. F. (1999) *Biochemistry 38*, 7131−7141.
22. Yang, X.-Y., Miles, E. W. (1993) *J. Biol. Chem. 268*, 22269−22272.
23. Ahmed, S. A., Ruvinov, S. B., Kayastha, A. M., and Miles, E. W. (1991) *J. Biol Chem. 266*, 21540−21557.
24. Rowlett, R., Yang, L. H., Ahmed, S. A., McPhie, P., Jhee, K. H., and Miles, E. W. (1998) *Biochemistry 37*, 2961−2968).
25. Fan, Y.-X., McPhie, P., and Miles, E. W. (2000) *J. Biol. Chem. 275*, 20302−20307.
26. Schneider, T. R., Gerhardt, E., Lee, M., Liang, P.-H., Anderson, K. S., and Schlichting, I. (1998) *Biochemistry 37*, 5394−5406.
27. Bahar, I, and Jernigan, R. L., (1999) *Biochemistry 38*, 3478−3490.
28. Kirschner, K., Weischet, W., and Wiskocil, R. L. (1975) in *Protein−Ligand Interactions* (Sund, H., and Blaver, G., Eds.) pp 27−44, Walter de Gruyter, Berlin.
29. Weischet, W. O., and Kirschner, K. (1976) *Eur. J. Biochem. 65*, 365−373.
30. Koerber, S. C., MacGibbon, A. K. H., Dietrich, H., Zeppezauer, M., and Dunn, M. F. (1983) *Biochemistry 22*, 3424−3431.
31. Drewe, W. F., Jr., and Dunn, M. F. (1985) *Biochemistry 24*, 3977−3987.
32. Drewe, W. F., Jr., and Dunn, M. F. (1986) *Biochemistry 25*, 2494−2501.
33. Brzovic, P. S., and Dunn, M. F. (1993), *Bioanalytical Instrumentation 37* (Suelter, C. H., Ed.) pp 191−273, J. Wiley and Sons, Inc., NY.
34. Brzovic, P. S., and Dunn, M. F. (1995) *Methods Enzymol. 246*, 168−201.
35. Roy, M., Keblawi, S., and Dunn, M. F. (1988) *Biochemistry 27*, 6698−6704.
36. Rhee, S., Miles, E. W., Davies, D. R. (1998) *J. Biol. Chem. 273*, 8553−8555.
37. Sachpatzidis, A., Dealwis, C., Lubetsky, J. B., Liang, P. H., Anderson, K. S., and Lolis, E. (1999) *Biochemistry 38*, 12665−12674.
38. Perutz, M. F. (1989) *Q. Rev. Biophysics 22*, 139−236.
39. Bloom, C. R., Kaarsholm, N. C., Ha, J. and Dunn, M. F. (1997) *Biochemistry 36*, 12759−12765.
40. Huang, Y., and Ackers, G. K. (1996) *Biochemistry 35*, 704−718.
41. Woehl, E. U., and Dunn, M. F. (1995) *Coord. Chem. Rev. 144*, 147−197.
42. Houben, K. F., and Dunn, M. F. (1990) *Biochemistry 29*, 2421−2429.
43. Houben, K. F., Kadima, W., Roy, M., and Dunn, M. F. (1989) *Biochemistry 28*, 4140−4147.
44. Rhee, S., Miles, E. W., Mozzarelli, A., Davies, D. R. (1998) *Biochemistry 37*, 10653−10659.